RSC Advances

This is an *Accepted Manuscript*, which has been through the Royal Society of Chemistry peer review process and has been accepted for publication.

Accepted Manuscripts are published online shortly after acceptance, before technical editing, formatting and proof reading. Using this free service, authors can make their results available to the community, in citable form, before we publish the edited article. This *Accepted Manuscript* will be replaced by the edited, formatted and paginated article as soon as this is available.

You can find more information about *Accepted Manuscripts* in the Information for Authors.

Please note that technical editing may introduce minor changes to the text and/or graphics, which may alter content. The journal's standard Terms & Conditions and the Ethical guidelines still apply. In no event shall the Royal Society of Chemistry be held responsible for any errors or omissions in this *Accepted Manuscript* or any consequences arising from the use of any information it contains.

ROYAL SOCIETY OF CHEMISTRY

www.rsc.org/advances

Facile synthesis of $Ni_{0.85}Se$ on Ni foam for high-performance asymmetric capacitor

Chao Gong, Miaoliang Huang*, Jinfang Zhang, Min Lai, Leqing Fan, Jianming Lin, Jihuai Wu

Engineering Research Center of Environment-Friendly Functional Materials, Ministry of Education; Institute of Materials Physical Chemistry, College of Materials Science and Engineering, Huaqiao University, Xiamen, Fujian, 361021, P. R. China

Abstract

$Ni_{0.85}Se$ was in situ grown on Ni foam via a facile hydrothermal process as a high-performance electrode for supercapacitors. The as-obtained $Ni_{0.85}Se$ electrode exhibited excellent electrochemical property with a higher specific capacitance of 1115 F g^{-1} (1.34 F cm^{-2}) and remarkable cycling stability (91.7% of the initial capacitance value remained after 1000 cycles). An asymmetric supercapacitor was fabricated successfully based on $Ni_{0.85}Se$ (positive electrode) and activated carbon (negative electrode). The $Ni_{0.85}Se$//AC ASC can expand the operating voltage as high as 1.6 V, led to an ultrahigh energy density of 32.2 Wh kg^{-1} at a power density of 789.6 W kg^{-1}. Further, the ASC had a highlight cycle performance (only 1.7% of C_T loss after 2000 cycles), it holds promise as the potential candidate for energy storage device.

*Corresponding Author, TEL: (+86) 592-6162255; E-mail: mlhuang2012@hotmail.com.

Address: College of Materials Science and Engineering, Huaqiao University, No.668, Jimei Road, Jimei Area, Xiamen, Fujian, 361021, P. R. China.

RSC Advances Accepted Manuscript

1. Introduction

In recent years, the energy crisis and resources shortage are becoming more and more serious with the rapid development of industry and economy. To develop clean and renewable energy as well as a suitable energy storage equipment is urgent. Supercapacitors or electrochemical capacitors have been widely concerned as next generation energy storage devices because of their superhigh power density, long cycling stability, rapid charge-discharge and non-pollution.[1-3] Depending on the storage charge mechanism, supercapacitors are classified into two types. One is electrical double-layer supercapacitor (EDLS), whose electrode material mostly includes carbon-based conducting porous materials. The other is the pseudocapacitor, also called the Faradic supercapacitor, which uses a rapid and reversible redox reaction to collect charges. In general, the pseudocapacitors by Faraday process possess much more specific capacitance than EDLSs.[4]

Although the supercapacitor can store hundreds or thousands of times more charge than conventional physical capacitor, the energy density of the supercapacitor is still lower compared to secondary battery.[5] Base on the formula for supercapacitor energy density: $E = 1/2CV^2$, the energy density can be improved by enhancing the operation voltage (V) and/or the specific capacitance (C).[6,7] One promising method to increase both the specific capacitance and operation voltage is to assemble asymmetric supercapacitor, which integrates the advantages of supercapacitors (rate, cycle life) and batteries (energy density), and expands operation voltage by using different electrode material in one system.[8,9] The key to fabricating asymmetric supercapacitor is to employ suitable materials for positive and negative electrode working in different potential windows in appropriate electrolyte.

RSC Advances Accepted Manuscript

At present, carbon-based materials are currently used as the negative electrode material, such as carbon nanotudes, carbon nanofibers, activated carbon and graphene are widely used in the asymmetric supercapacitor.[10-13] Among them, activated carbon with high specific surface area, fine electrical conductivity, good chemical stability and easy preparation, has been used commonly.[6] The positive electrode materials mainly consist of transition metal oxides/hydroxides and sulfides, and conductive polymers. Such as RuO_2[14], MnO_2[15], Mn_3O_4[16], CoO[17], Ni_3S_2[18] and Co_9S_8[19] et al.

However, comparing with the transition metal oxides and sulfides, research on transition metal selenide as the positive electrode materials is relatively limited. Wang et al.[20] synthesized 3D hierarchical $GeSe_2$ nanaostructures with a specific capacitance of 300 F g^{-1} via a chemical vapor deposition method. Zhang and co-workers[21] successfully fabricated two-dimensional tin selenide nanostructures for all-solid-state supercapacitors with the specific capacitances of 168 F g^{-1} ($SnSe_2$) and 228 F g^{-1} (SnSe). Recently, Banerjee et al.[22] fabricated hollow $Co_{0.85}Se$ nanowire array by chemical hydrothermal process, which exhibited high pseudocapacitive property with an areal capacitance of 929.5 mF cm^{-2} at 1 mA cm^{-2} and high durability.

Among them, nickel selenide as an important transition metal chalcogenide, exhibits interesting electronic and magnetic properties[23]. In addition, it has been proven with superior electrochemical performance, which can serve as the electrode material for Li ion battery[24] and Pt-free counter electrode for dye-sensitized solar cell[25]. But few papers are contributed to the research on the nickel selenide for application in supercapacitors.

In this study, we successfully prepared $Ni_{0.85}Se$ on Ni foam via an in-situ growth process.

RSC Advances Accepted Manuscript

Ni foam has 3D porous frameworks structure, high surface area, good conductive, and low cost, and has been often used as current collector/or supporter.[26,27] The electrode of $Ni_{0.85}Se$ reveals prominent pseudocapacitive property with higher specific capacitance of 1115 F g^{-1} (1.34 F cm^{-2}) at 1 A g^{-1}. Moreover, so as to extend voltage window, we assemble asymmetric supercapacitor (ASC) by employing $Ni_{0.85}Se$ as positive electrode and activated carbon as negative electrode. The ASC can be cycled stably with a high voltage of 1.6 V and demonstrates superior energy density of 32.2 Wh kg^{-1} with excellent cycling stability.

2. Experimental

2.1 Materials

Polytetrafluoroethylene (PTFE) aqueous solution (60wt%), anhydrous ethanol and $N_2H_4 \cdot H_2O$ (80wt%) were from Sinopharm Chemical Reagent Co.,Ltd. Se powder and $NiCl_2 \cdot 6H_2O$ were purchased from Shanghai Aladdin Reagent. Activated carbon (AC) (surface area 2167 m^2 g^{-1}) was from Fuzhou Yihuan Co.,Ltd. Ni foam (porosity 87.3%) was from Changsha Liyuan Co.,Ltd. All materials were commercially available and employed without further purification.

2.2 Preparation of $Ni_{0.85}Se$ electrode

One-step hydrothermal process was used for growing $Ni_{0.85}Se$ on Ni foam. The main steps were described as following: 0.2 mmol $NiCl_2 \cdot 6H_2O$ was added into a 100 ml Teflon-lined autoclave and dissolved in 55 ml deionized water. 0.24 mmol selenium powder was put into the autoclave to form a homogeneous solution. Then 15 ml $N_2H_4 \cdot H_2O$ was added and stirred for 20 min. After stirring, 5 pieces of washed Ni foam (1 cm^2) were immersed into reaction solution. The autoclave was airtight and kept at 160□ for 12 h in an oven. After

RSC Advances Accepted Manuscript

hydrothermal process, black samples were obtained from the autoclave. Finally, the samples were washed (with DI water and absolute ethanol), dried and the $Ni_{0.85}Se$ electrode was obtained. The mass of $Ni_{0.85}Se$ on Ni foam is about 1.2 mg cm^{-2}, and its porosity is about 85.4%.

2.3 Preparation of activated carbon electrode

Activated carbon (AC) (80 wt%), acetylene black (10 wt%) and PEFT aqueous solution (10 wt%), were mixed with a little ethanol to form a homogeneous paste. The paste was pressed into a thin sheet. Then, the thin sheet was pressed onto a nickel net. After being dried at 70 □ for 12 h, an AC electrode was obtained.

2.4 Material characterization

The phase of prepared samples was investigated by a SmartLab X-Ray diffractometer using a Cu Kα radiation (λ=1.5418Å) at a scan rate of 10°min^{-1} over 2θ range from 20 to 70°(Rigaku D/MAX- RB, Japan). The morphology of the products was characterized by a field emission scanning electron microscopy (FESEM, HITACHI SU8010). The porosity of Ni foam and $Ni_{0.85}Se$-coated Ni foam were tested by a mercury intrusion porosimetry (quantachrome , PoreMaster-60).

2.5 Electrochemical characterization

The electrochemical properties of $Ni_{0.85}Se$ electrode were studied with a three-electrode configuration in 3 M KOH electrolyte. The counter electrode employed a platinum sheet and HgO/Hg was applied for the reference electrode. $Ni_{0.85}Se$//AC asymmetric supercapacitor (ASC) was fabricated by employing $Ni_{0.85}Se$ and AC as positive and negative electrode, respectively. A double electrode system in 3 M KOH was employed to characterize the

RSC Advances Accepted Manuscript

electrochemical performance of ASC. Cyclic voltammetry (CV), electrochemical impedance spectroscopy (EIS) and galvanostatic charge-discharge (GCD) tests were carried on CHI660E electrochemical workstation.

The specific capacitances of the supercapacitor were estimated from GCD curves based on eqn (1), (2)[28,32]

$$C_m = \frac{I \times \Delta t}{m \times \Delta V} \quad (1)$$

$$C_s = \frac{I \times \Delta t}{S \times \Delta V} \quad (2)$$

The energy density and power density of ASC were evaluated by eqn (3) and (4)[28], respectively.

$$E = \frac{1}{2} C_m (\Delta V)^2 \quad (3)$$

$$P = \frac{E}{\Delta t} \quad (4)$$

Wherein C_m (F g^{-1}) is the mass specific capacitance and C_s (F cm^{-2}) is the area specific capacitance, I (A), Δt (s), m (g), S and ΔV (V) represents the discharge current, the discharge time, the mass of electroactive material, the area of electroactive materials and the voltage variety during the discharge process after potential drop, respectively. E (Wh kg^{-1}) is energy density and P (W kg^{-1}) is power density.

3. Results and discussion

RSC Advances Accepted Manuscript

3.1 Characterization of electrode materials

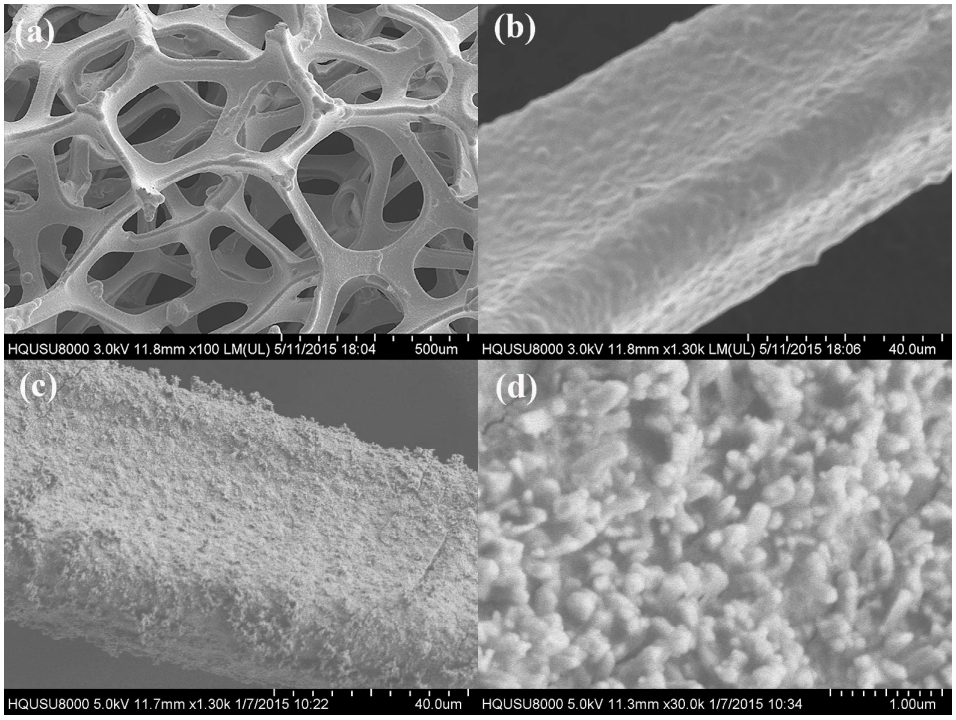

Fig. 1 FESEM images of $Ni_{0.85}Se$ on Ni foam and pure Ni foam.

(a) (b) pure Ni foam, (c) (d) $Ni_{0.85}Se$ on Ni foam.

FESEM was employed to investigate the morphology of as-synthesized samples. Fig. 1 (a,b) and Fig. 1(c,d) show images of pure Ni foam and $Ni_{0.85}Se$ on Ni foam under the different magnifications. From Fig. 1(a,b), it can be seen that pure Ni foam has a 3D porous frameworks and its surface is smooth, and then became rough after growing $Ni_{0.85}Se$, as shown in Fig. 1(c). $Ni_{0.85}Se$ can be observed and has a homogeneous distribution on Ni foam surface in Fig. 1(d). The high dispersion of $Ni_{0.85}Se$ on 3D porous frameworks Ni foam will provide more active sites for Faradic redox action, facilitate the electrolyte deep penetration within electrode, effective contact on the surface of the electrode, accelerate ion and electron transfer in the interface between the electrolyte and $Ni_{0.85}Se$, resulting in the excellent

RSC Advances Accepted Manuscript

electrochemical performance.[27,29]

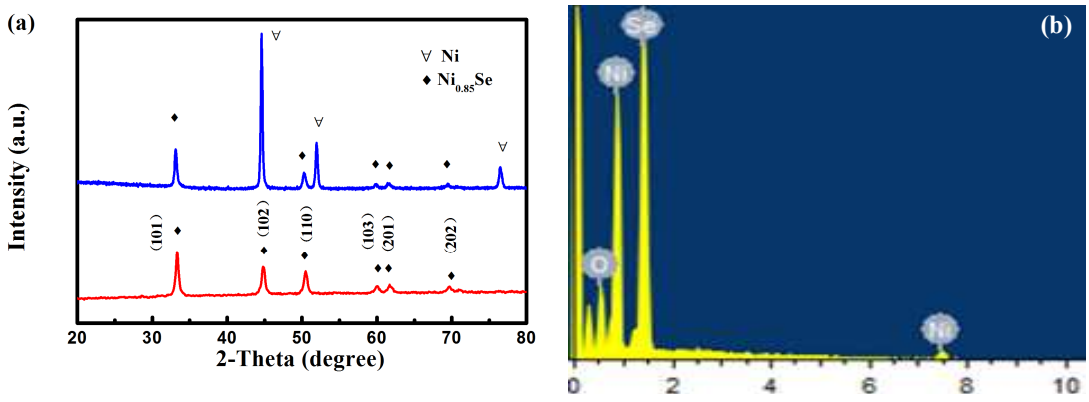

Fig. 2(a) XRD spectrum of $Ni_{0.85}Se$ and $Ni_{0.85}Se$ on Ni foam; (b) EDS pattern of $Ni_{0.85}Se$

Fig. 2(a) shows the XRD patterns of as-synthesized $Ni_{0.85}Se$ samples on Ni foam (blue curve) and pure $Ni_{0.85}Se$ (red curve) which detached from the Ni foam substrate via long time of ultrasonic process. Except for three strong peaks (44.7°, 52.1° and 76.5°) from the Ni foam substrate, all of peak positions can be completely indexed to $Ni_{0.85}Se$ (JCPDS No.18-0888). The result of XRD declares that $Ni_{0.85}Se$ has successfully grown on Ni foam without other by-product. Fig. 2(b) displays the EDS pattern of $Ni_{0.85}Se$, it can be seen that except a little oxygen signal (may be from moisture and oxygen adsorbed on the surface of sample[22]), no extra elements are found.

3.2 Electrochemical performance of $Ni_{0.85}Se$ electrode

The electrochemical characteristics of $Ni_{0.85}Se$ electrode were investigated using Cyclic voltammetry (CV) tests. Fig. 3(a) exhibits the CV curves of $Ni._{085}Se$ electrode measured in 3 M KOH solution with different scan rates. Obviously, a pair of redox peaks appear in each curve with the scan rate changes from 5 to 100 mV s^{-1}. This is attributed to that the electrochemical capacitance of $Ni_{0.85}Se$ electrode mainly comes from pseudocapacitance

RSC Advances Accepted Manuscript

rather than the electric double-layer capacitance, which is similar to rectangle.[27,30] With the increase of the scan rate, the anodic and cathodic peaks shift toward higher and lower voltage, respectively, and the shapes of CV curves have no obviously distortion. All curves have good symmetry in Fig. 3(a), indicating that the electrode of $Ni_{0.85}Se$ possesses excellent reversibility and capacitive behavior.[17,18] The electrochemical mechanism of $Ni_{0.85}Se$ electrode is still not totally understood, which probably executes through the electrode interface adsorption and desorption of hydroxyl ions in alkaline electrolyte.[22]

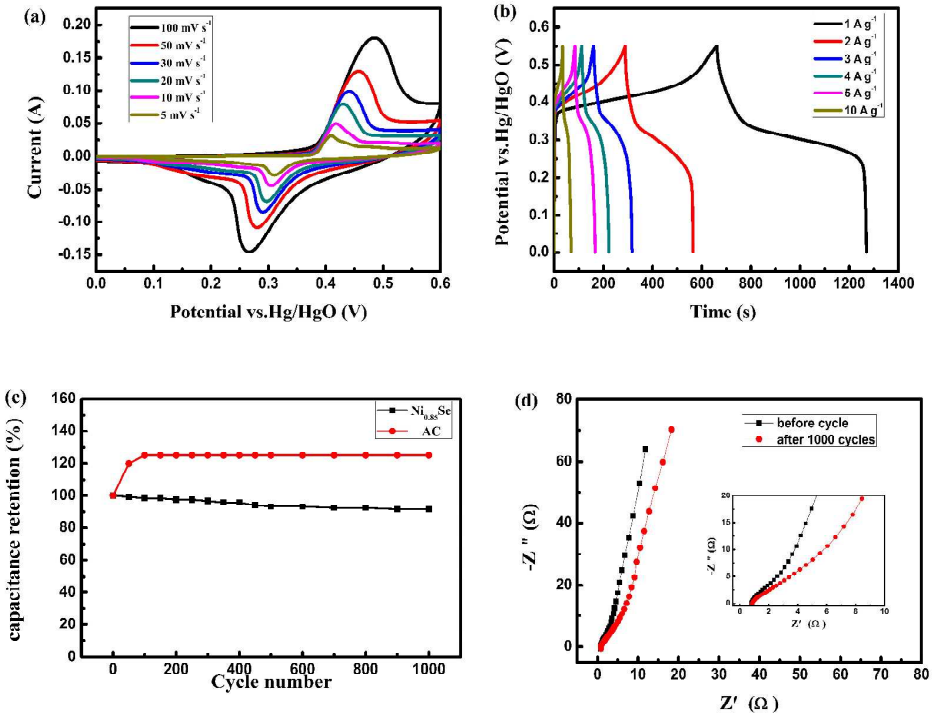

Fig. 3 Electrochemical performances of the $Ni_{0.85}Se$ electrodes:(a) CV curves at different scan rates; (b) GCD curves at different current densities; (c) cycling performances of the $Ni_{0.85}Se$ and AC electrode during 1000 cycles at current density of 5 A g^{-1}. (d) EIS measured at the open circuit potential in the frequency range from 0.01 to 10^5 Hz.

RSC Advances Accepted Manuscript

To further study the electrochemical property of $Ni_{0.85}Se$ electrode, the galvanostatic charge-discharge measurement was performed on with different current densities in the voltage change from 0 to 0.55 V (vs Hg/HgO), as shown in Fig. 3(b). A pair of obvious charge-discharge platforms can be observed at each curve, consisted well with a pair of redox peaks in CV curves, which is further evidence of the pseudocapacitance performance of the $Ni_{0.85}Se$ electrode.[31] A sequence of specific capacitances under various current densities were evaluated based on eqn (1) (2). The mass specific capacitance C_m and the area specific capacitance C_s of $Ni_{0.85}Se$ electrode with different current densities were evaluated and listed in Table 1.

Table 1 The specific capacitance of the $Ni_{0.85}Se$ electrode

The current density (A g^{-1})	C_m (F g^{-1})	C_s (F cm^{-2})
1	1115.0	1.34
2	1023.6	1.23
3	863.9	1.04
4	815.3	0.98
5	773.7	0.93
10	662.3	0.79

As a rule, increasing in current density will lead to a reduction of capacitance value due to the incremental voltage drop and active material can not fully participate in redox reaction.[27] Fortunately, as the current density is up to 10 A g^{-1}, the specific capacitance of the electrode still maintains higher, reaches to 662.3 F g^{-1} (0.79 F cm^{-2}), indicating that the $Ni_{0.85}Se$ electrode has a good rate capacitive performance, which is significance for the practical application of the electrode material for supercapacitors.[22]

RSC Advances Accepted Manuscript

A continuous charging and discharging process was used to evaluate the cyclic stability of $Ni_{0.85}Se$ electrode, and the results are shown in Fig. 3(c) (black curve). Furthermore, in order to study the cycle stability of the asymmetric supercapacitor, the life cycle plot of AC electrodes was also performed, and shown in Fig. 3(c) (red curve). Under a constant current density of 5 A g^{-1}, the electrode was carried out for 1000 times charge-discharge tests in 3 M KOH solution with three-electrode construction. The electrode capacitance value remains 91.7% of initial specific capacitance after 1000 times cycles, indicating that $Ni_{0.85}Se$ is an ideal electrode material for supercapacitor with excellent cycling stability and electrochemical properties, which is ascribed to the $Ni_{0.85}Se$ directly grown on Ni foam conductive substrate, avoiding the "dead surface" of the traditional slurry-derived electrode and benefitting to the charge fast transfer between the interface of $Ni_{0.85}Se$ electrode and Ni foam, and electrolyte penetration and ion diffusion in porous Ni foam.[29] EIS of the $Ni_{0.85}Se$ electrode before and after 1000 cycles were also measured. The Nyquist impedance plots of the $Ni_{0.85}Se$ electrode are shown in Fig. 3(d), which consist of a semicircle and a straight line at the high- and low-frequency region, respectively. Distinctly, the internal and charge-transfer resistance of the electrodes before and after 1000 cycles at the high-frequency region are almost kept same. But at the low-frequency region, there is a slight reduction in the slope of Nyquist impedance plots after 1000 charge-discharge tests, indicating that the diffusive resistance of electrode increases, which is reason why the specific capacitance decreases.

3.3 The effect of loading amount of $Ni_{0.85}Se$ on specific capacitance

In order to study the effect of loading amount of $Ni_{0.85}Se$ on specific capacitance, we prepared six samples of $Ni_{0.85}Se$ on Ni foam with different loading of $Ni_{0.85}Se$ by controlling

RSC Advances Accepted Manuscript

the amount of reaction materials, the loading of $Ni_{0.85}Se$ is about 0.7, 1.2, 1.8, 2.5, 3.2 and 4.1 mg, respectively. Fig.4(a) shows the charge-discharge curves with different loading of $Ni_{0.85}Se$ on Ni foam at a current density of 1 A g^{-1}. The mass specific capacitance (C_m) was calculated and the results were shown in Fig.4(b). At first, the C_m of electrode increased along with the load of $Ni_{0.85}Se$ improved, and reached the maximum value when the load is 1.2 mg, which is attributed to the increase of the load of $Ni_{0.85}Se$ on Ni foam can provide more active sites. However, with the load further increased from 1.2 to 4.1 mg, the C_m of electrode has a great attenuation from 1115 to 279.3 F g^{-1}. These results are probably attributed to the following reasons. Firstly, with the increase of load of $Ni_{0.85}Se$, the outer $Ni_{0.85}Se$ can not directly contact with the Ni foam substrate which hindered electronic transmission. In addition, the over loading will influence the penetration of electrolyte in inner active material, and resulting in the decrease of specific capacitance.

RSC Advances Accepted Manuscript

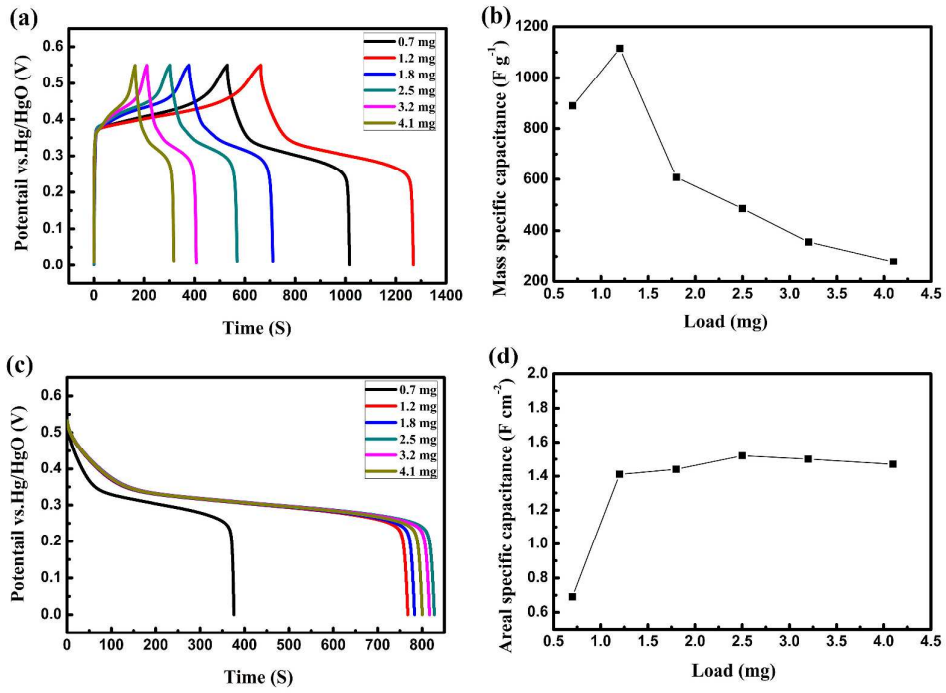

Fig. 4(a) Charge-discharge curve of different loading of $Ni_{0.85}Se$ on Ni foam at a current density of 1 A g^{-1}; (b) The mass specific capacitance of different load of $Ni_{0.85}Se$ on Ni foam; (c) Discharge curve of different load of $Ni_{0.85}Se$ on Ni foam at a current density of 1 mA cm^{-2}; (d) The area specific capacitance of different load of $Ni_{0.85}Se$ on Ni foam.

In addition, Fig. 4(c) shows the discharge curve of different load of $Ni_{0.85}Se$ on Ni foam at a current density of 1 mA cm^{-2}, the corresponding area specific capacitance (C_s) for different load of were shown in Fig. 4(d). Firstly, the C_s of electrode has significantly increased when the load of $Ni_{0.85}Se$ increases from 0.7 to 1.2 mg. And when the load of $Ni_{0.85}Se$ increases from 1.2 to 4.1 mg, the C_s of electrode is only a small change from 1.41 to 1.47 F cm^{-2}. Obviously, when the load of $Ni_{0.85}Se$ is greater than 1.2 mg, the C_s of electrode increased only in a small scale, however, the C_m of electrode has a highly attenuation.

RSC Advances Accepted Manuscript

Therefore, in this experimental condition, the optimal load of $Ni_{0.85}Se$ on Ni foam substrate is about 1.2 mg.

3.4 Asymmetric supercapacitor

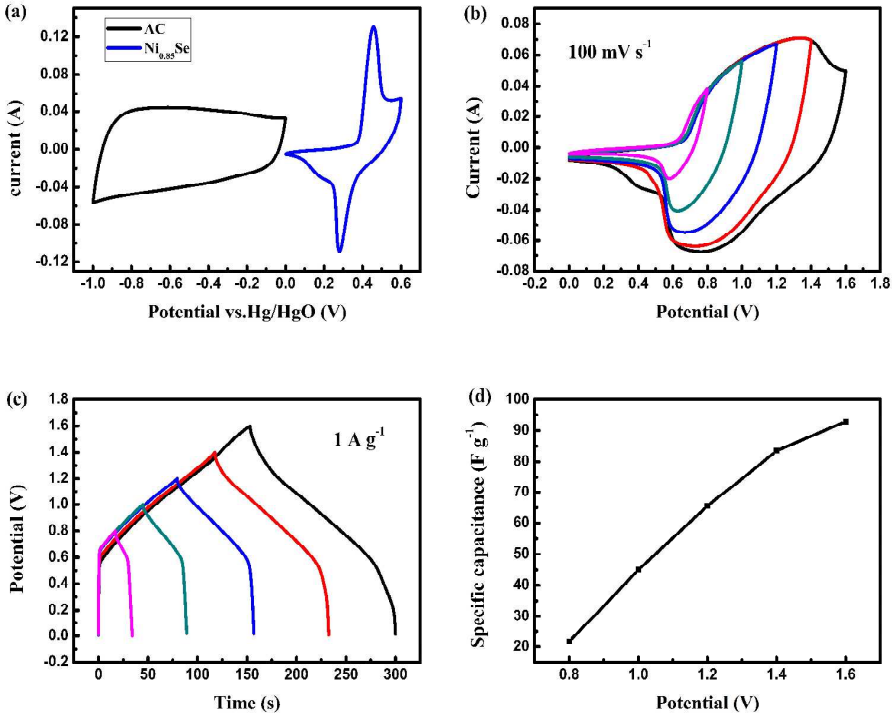

Fig.5(a) CV curves of the $Ni_{0.85}Se$ and AC electrodes collected at 50 mV s^{-1} in a three-electrode system; (b) CV curves of $Ni_{0.85}Se$//AC asymmetric supercapacitor at different potential windows at 100 mV s^{-1}; (c) GCD curves of the ASC device obtained at different potential windows at a constant current density of 1 A g^{-1}. (d) C_m of the ASC as a function of potential window.

Above experimental results indicate that $Ni_{0.85}Se$ electrode has high specific capacitance and excellent cycle stability, signifying that it is a promising positive electrode material of asymmetric supercapacitor (ASC). Fig. 5(a) shows complementary CV curves of $Ni_{0.85}Se$ and

RSC Advances Accepted Manuscript

AC electrode when assessed in 3 M KOH aqueous solution with three-electrode cell. The two electrode materials occupy different voltage window, the potential window of $Ni_{0.85}Se$ and AC electrodes are 0 to 0.6 V (vs. Hg/HgO) and -1 to 0 V (vs. Hg/HgO) , respectively. Hence, the potential window can be extended to 1.6 V by assembling an asymmetric supercapacitor with AC as the negative electrode and $Ni_{0.85}Se$ as the positive electrode.[9,30] In order to obtain stable and efficient ASC, the charges of two electrodes must be kept in balance. Positive and negative electrodes are matched by the mass balance method[33].

$$R = \frac{m^-}{m^+} = \frac{C_m^+ \Delta V^+}{C_m^- \Delta V^-} \approx \frac{8}{3} \qquad (5)$$

Where m^+ and m^- are the mass of activated materials, C_m^+ (1115 F g^{-1}, 1 A g^{-1}) and C_m^- (234.3 F g^{-1}, 1 A g^{-1}) represent specific capacitance, and ΔV^+ and ΔV^- are the potential windows of positive and negative electrodes, respectively.

Fig. 5(b) presents the CV curves of ASC under various potential windows from 0.8 V to 1.6 V at a scan rate of 100 mV s^{-1}. With the increase of voltage, all curves remain similarity and there is no sign of water splitting.[22] Thus, the ASC can be operated at a high voltage of 1.6 V and kept stable electrochemical performance. According to the eqn (1) and the GCD curves of different potential windows (Fig. 5(c)), the specific capacitance of ASC under various voltage from 0.8 to 1.6 V were calculated and the results are demonstrated in Fig. 5(d). When the voltage window extended from 0.8 to 1.6 V, the C_m of ASC improved sharply from 21.7 to 92.9 F g^{-1}, and energy densities change from 1.8 to 32.2 Wh kg^{-1} are calculated by eqn (3), which means that increasing the working voltage of asymmetric supercapacitor is the key factor to obtaining high-performance storage device.[6,9]

RSC Advances Accepted Manuscript

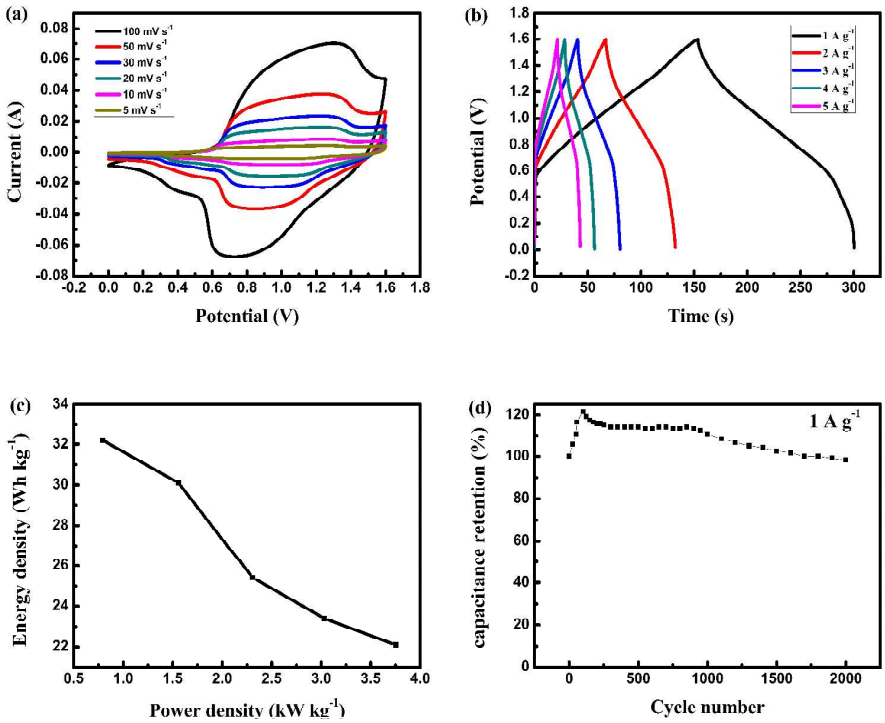

Fig. 6 Electrochemical performance of the $Ni_{0.85}Se$//AC ASC: (a) CV curves at different scan rates; (b) GCD curves at different current densities; (c) Ragone plot of ASC; (d) cycling performances during 2000 cycles at current density of 1 A g^{-1}.

For the purpose of further understanding the performance of ASC, other electrochemical tests were carried out. The CV measurements with various sweep rates range from 5 to 100 mV s^{-1}, all curve shapes are well maintained, and without obvious sign of distortion even at high scan rate of 100 mV s^{-1}, as shown in Fig. 6(a). The GCD measurements of ASC were executed at different current densities changed from 1 to 5 A g^{-1} in 3 M KOH solution with two-electrode system, as shown in Fig.6(b). The specific capacitances of the $Ni_{0.85}Se$//AC ASC were evaluated based on the eqn (1) (2). The GCD curves also were employed for calculating the energy and power densities of the $Ni_{0.85}Se$//AC asymmetric supercapacitor.

RSC Advances Accepted Manuscript

The calculated results are listed in table 2.

Table 2 The electrochemical parameters of $Ni_{0.85}Se$//AC ASC

The current density (A g^{-1})	C_m (F g^{-1})	C_s (mF cm^{-2})	E (Wh kg^{-1})	P (W kg^{-1})
1	92.9	272.5	32.2	789.6
2	89.3	261.9	30.1	1556.9
3	77.2	226.5	25.4	2309.1
4	73.4	215.3	23.4	3030.2
5	70.7	207.4	22.1	3752.8

The highest capacitance value of 92.9 F g^{-1} (272.5 mF cm^{-2}) was achieved at 1 A g^{-1}, and 76.1% initial capacitance value was kept when the current density changed from 1 to 5 A g^{-1}. The high rate performance of both $Ni_{0.85}Se$ and AC led to above result. As the current density ranging from 1 to 5 A g^{-1}, the Ragone plot of ASC is presented in Fig. 6(c). The highest energy and power densities of ASC attained 32.2 Wh kg^{-1} and 3752.8 W kg^{-1}, respectively. In addition, the cycling stability of ASC was assessed at a constant current density of 1 A g^{-1}. As shown in Fig. 6(d), the capacitance increased to 121.7% of the initial value after 100 cycles, this phenomenon is similar to the cycle life plot of AC electrode in Fig. 3(c)), which is due to the gradually activation of the active sites of the thin sheet AC electrode which was fabricated by the traditional Decal method.[27,34] After 2000 cycles, the ASC exhibited excellent stability with 98.3% retention of capacitance, it is attributed to the prominent electrochemical stability of both activated carbon and $Ni_{0.85}Se$ electrodes.

4. Conclusion

$Ni_{0.85}Se$ was successfully fabricated on Ni foam by one-step hydrothermal process. It is

RSC Advances Accepted Manuscript

used as electrode material for supercapacitor, and possesses outstanding electrochemical characteristics and cycling stability. At the current density of 1 A g^{-1}, the $Ni_{0.85}Se$ electrode shows a higher capacitance value of 1115 F g^{-1} (1.34 F cm^{-2}). The $Ni_{0.85}Se$ was used as a positive electrode of an asymmetric supercapacitor with AC as negative electrode, the maximum energy density of ASC reaches up to 32.2 Wh kg^{-1} with a power density of 789.6 W kg^{-1}. The results exhibit that $Ni_{0.85}Se$ is a promising electrode material for application in supercapacitor.

Acknowledgements

This work was jointly supported by the National Natural Science Fund of China (No. U1205112) and Provincial Natural Science Foundation of Fujian, China (No. D0010011).

Reference

1. P. Simon and Y. Gogotsi, *Nat. Mater.*, 2008, **7**, 845-854.

2. Frackowiak E and Béguin F, *Carbon*, 2001, **39**, 937-950.

3. Y. W. Zhu, S. T. Murali, M. D. Stoller, K. J. Ganesh, W. W. Cai, P. J. Ferreira, A. Prikel, R. M. Wallace, K. A. Cychosz, M. Thommes, D. Su, E. A. Stach and R. S. Ruoff, *Science*, 2011, **332**, 1537-1541.

4. N. Katsuhiko and S. Patrice, *J. Electrochem. Soc.*, 2008, **17**, 34-37.

5. Z. Tang, C. H. Tang and H. Gong, *Adv. Funct. Mater.*, 2012,**22**, 1272-1278.

6. Z. J. Fan, J. Yan, T. Wei, L. J. Zhi, G. Q. Ning, T. Y. Li and F. Wei, *Adv. Funct. Mater.*, 2011, **21**, 2366–2375.

7.V. Khomenko, E. Raymundo-Piñero and F. Béguin, *J. Power Sources*, 2010, **195**, 4234-4241.

8. L. Demarconnay, E. Raymundo-Piñero and F. Béguin, *J. Power Sources*, 2011, **196**,

RSC Advances Accepted Manuscript

580-586.

9. L. Q. Fan, G. J. Liu, J. H. Wu, L Liu, J. M. Lin and Y. L. Wei, *Electrochim. Acta*, 2014, **137**, 26-33.
10. F. X. Wang, S. Y. Xiao, Y. Y. Hou, C. L. Hu, L. L. Liu and Y. P. Wu, *RSC Adv.*, 2013, **3**, 13059-13084.
11. C. S. Dai, P. Y. Chien, J. Y. Lin, S. W. Chou, W. K. Wu, P. H. Li, K. Y. Wu and T. W. Lin, *ACS Appl. Mater. Interfaces*, 2013, **5**, 12168-12174.
12. J. L. Shen, C. Y. Yang, X. W. Li and G. C. Wang, *ACS Appl. Mater. Interfaces*, 2013, **5**, 8467-8476.
13. G. H. Yu, L. B. Hu, M. Vosgueritchian, H. L. Wang, X. Xie, J. R. McDonough, X. Cui, Y. Cui and Z. N. Bao, *Nano Lett.*, 2011, **11**, 2905-2911.
14. Y. G. Wang, Z. D. Wang and Y. Y. Xia, *Electrochim. Acta*, 2005, **50**, 5641-5646.
15. Z. S. Wu, W. Ren, D. W. Wang, F. Li, B. L. Liu and H. M. Cheng, *ACS Nano*, 2010, **4**, 5835-5842.
16. Y. Li and X. M. Li, *RSC Adv.*, 2013, **3**, 2398-2403.
17. C. Zhou, Y. Zhang, Y. Li and J. P. Liu, *Nano lett.*, 2013, **13**, 2078-2085.
18. G. Debasis and K. D. Chapal, *ACS Appl. Mater. Interfaces*, 2015, **7**, 1122-1131.
19. R. B. Rakhi, N. A. Alhebshi, D. H. Anjum and H. N. Alshareef, *J. Mater. Chem. A*, 2014, **2**, 16190-16198.
20. X. F. Wang, B. Liu, Q. F. Wang, W. F. Song, X. J. Hou, D. Chen, Y. B. Cheng and G. Z. Shen, *Adv. Mater.*, 2013, **25**, 1479-1486.
21. C. L. Zhang, H. H. Yin, M. Han, Z. H. Dai, H. Pang, Y. L. Zheng, Y. Q. Lan, J. C. Bao and J. M. Zhu, *ACS Nano*, 2014, **4**, 3761-3770.
22. A. Banerjee, S. Bhatnagar, K. K. Upadhyay, P. Yadav and S. Ogale, *ACS Appl. Mater. Interfaces*, 2014, **6**, 18844-18852.

RSC Advances Accepted Manuscript

23. Z. B. Zhuang, Q. Peng, J. Zhuang, X. Wang and Y. D. Li, *Chem. Eur. J.*, 2006, **12**, 211-217.

24. L. W. Mi, H. Sun, Q. Ding, W. H. Chen, C. T. Liu, H. W. Hou, Z. Zheng and C. Y. Shen, *Dalton Trans.*, 2012, **41**, 12595-12600.

25. F. Gong, H. Wang, X. Xu, G. Zhou and Z. S. Wang, *J. Am. Chem. Soc.*, 2012, **134**, 10953-10958.

26. V. H. Nguyen, J. Shim, *Electrochim. Acta*, 2015, **166**, 302-309.

27. X. H. Xiong, D. Ding, D. C. Chen, G. Waller, Y. F. Bu, Z. X. Wang and M. L. Liu, *Nano Energy*, 2015, **11**, 154-161.

28. T. W. Lin, C. S. Dai and K. C. Hung, *Sci. Rep.*, 2014, **4**, 7274-7274.

29. J. H. Huang, P. P. Xu, D. X. Cao, X. B. Zhou, S. N. Yang, Y. J. Li and G. L. Wang, *J. Power Sources*, 2014, **246**, 371-376.

30. H. C. Chen, J. J. Jiang, L. Zhang, T. Qi, D. D. Xia and H. Z. Wan, *J. Power Sources*, 2014, **248**, 28-36.

31. T. Wang, Y. Guo, B. Zhao, S. H. Yu, H. P. Yang D. Lu, X. Z. Fu, R. Sun and C. P. Wong, *J. Power Sources*, 2015, **286**, 371-379.

32. J. P. Wang, S. L. Wang, Z. C. Huang and Y. M. Yu, *J. Mater. Chem. A*, 2014, **2**, 17595-17601.

33. V. Khomenko, E. Raymundo-Pinero and F. Béguin, *J. Power Sources*, 2006, **153**, 183-190.

34. C. Z. Yuan, X. G. Zhang, L. H. Su, B. Gao and L. F. Shen, *J. Mater. Chem.*, 2009, **32**, 5772-5777.

RSC Advances Accepted Manuscript

Figure Captions

Fig .1 FESEM images of $Ni_{0.85}Se$ on Ni foam and pure Ni foam. (a) (b) pure Ni foam, (c) (d) $Ni_{0.85}Se$ on Ni foam.

Fig .2(a) XRD patterns of $Ni_{0.85}Se$ and $Ni_{0.85}Se$ on Ni foam; (b) EDS pattern of $Ni_{0.85}Se$.

Fig. 3 Electrochemical performances of the $Ni_{0.85}Se$ electrodes:(a) CV curves at different scan rates; (b) GCD curves at different current densities; (c) cycling performances of the $Ni_{0.85}Se$ and AC electrode during 1000 cycles at current density of 5 A g^{-1}. (d) EIS measured at the open circuit potential in the frequency range from 0.01 to 10^5 Hz.

Fig. 4(a) Charge-discharge curve of different loading of $Ni_{0.85}Se$ on Ni foam at a current density of 1 A g^{-1}; (b) The mass specific capacitance of different load of $Ni_{0.85}Se$ on Ni foam; (c) Discharge curve of different load of $Ni_{0.85}Se$ on Ni foam at a current density of 1 mA cm^{-2}; (d) The area specific capacitance of different load of $Ni_{0.85}Se$ on Ni foam.

Fig.5(a) CV curves of the $Ni_{0.85}Se$ and AC electrodes collected at 50 mV s^{-1} in a three-electrode system; (b) CV curves of $Ni_{0.85}Se$//AC asymmetric supercapacitor at different potential windows at 100 mV s^{-1}; (c) GCD curves of the ASC device obtained at different potential windows at a constant current density of 1 A g^{-1}. (d) C_T of the ASC as a function of potential window.

Fig.6 Electrochemical performance of the $Ni_{0.85}Se$//AC ASC: (a) CV curves at different scan rates; (b) GCD curves at different current densities; (c) Ragone plot of ASC; (d) cycling performances during 2000 cycles at current density of 1 A g^{-1}.

Table captions

Table 1 The specific capacitance of the $Ni_{0.85}Se$ electrode.

Table 2 The electrochemical parameters of $Ni_{0.85}Se$//AC ASC.

RSC Advances Accepted Manuscript